SANDIA REPORT

SAND2014-19498
Unlimited Release
Printed November 2014

Viscoelastic Material Inversion using SIERRA/SD and ROL

Timothy Walsh, Wilkins Aquino, Denis Ridzal, Drew Kouri,
Bart van Bloemen Waanders, Angel Urbina

Prepared by
Sandia National Laboratories
Albuquerque, New Mexico 87185 and Livermore, California 94550

Sandia National Laboratories is a multiprogram laboratory managed and operated by Sandia Corporation, a wholly owned subsidiary of Lockheed Martin Corporation, for the United States Department of Energy's National Nuclear Security Administration under Contract DE-AC04-94AL85000.

Issued by Sandia National Laboratories, operated for the United States Department of Energy by Sandia Corporation.

Available to DOE and DOE contractors from
U.S. Department of Energy
Office of Scientific and Technical Information
P.O. Box 62
Oak Ridge, TN 37831

Telephone: (865) 576-8401
Facsimile: (865) 576-5728
E-Mail: reports@adonis.osti.gov
Online ordering: http://www.osti.gov/bridge

Available to the public from
U.S. Department of Commerce
National Technical Information Service
5285 Port Royal Rd
Springfield, VA 22161

Telephone: (800) 553-6847
Facsimile: (703) 605-6900
E-Mail: orders@ntis.fedworld.gov
Online ordering: http://www.ntis.gov/help/ordermethods.asp?loc=7-4-0#online

SAND2014-19498
Unlimited Release
Printed November 2014

Viscoelastic Material Inversion using SIERRA/SD and ROL

Timothy Walsh
Computational Solid Mechanics and Structural Dynamics
Sandia National Laboratories
P.O. Box 5800
Albuquerque, NM 87185-0845 tfwalsh@sandia.gov

Wilkins Aquino
Department of Civil and Environmental Engineering
Duke University
Durham, NC

Denis Ridzal, Drew Kouri, Bart van Bloemenn Waanders
Optimization and Uncertainty Quantification
Sandia National Laboratories
P.O. Box 5800
Albuquerque, NM 87185-1320

Angel Urbina
Verification and Validation, UQ
Sandia National Laboratories
P.O. Box 5800
Albuquerque, NM 87185-1320

Abstract

In this report we derive frequency-domain methods for inverse characterization of the constitutive parameters of viscoelastic materials. The inverse problem is cast

in a PDE-constrained optimization framework with efficient computation of gradients and Hessian vector products through matrix free operations. The abstract optimization operators for first and second derivatives are derived from first principles. Various methods from the Rapid Optimization Library (ROL) are tested on the viscoelastic inversion problem. The methods described herein are applied to compute the viscoelastic bulk and shear moduli of a foam block model, which was recently used in experimental testing for viscoelastic property characterization.

Contents

Figures

1 Introduction

Predicting material properties from experimental measurements is a pervasive need in engineering systems, and spans multiple physics such as elasticity and viscoelasticity [1, 2, 3, 4, 5, 6, 7] as well as thermal analysis, and electromagnetics [8]. In all cases the inverse methodologies can be used to reconstruct the missing material parameters from direct experimental measurements. In contrast to previous approaches that have been based on time domain formulations, in this report we derive a frequency-domain formulation for the material inversion.

Modeling damping in structural systems is a long-standing research problem in structural dynamics. For Sandia-specific applications, the damping occurs in mechanical joints and interfaces due to friction effects, as well as in viscoelastic foams that are used to encapsulate certain structural components. These foams are viscoelastic materials, and thus provide both stiffness and damping in the overall structural response. However, their consitutive parameters often show significant variation from sample to sample, which introduces uncertainty into the finite element model. In this report we present a method for computing the parameters of these viscoelastic foams *in situ*, using measured accelerometer data from experiments. This has the advantage of computing the parameters of a given foam material as it is embedded in the structural system, rather than relying on test samples and the corresponding sample-to-sample variability.

We will adopt a PDE-constrained optimization approach to the problem. We break the optimization formulation into a set of abstract operators involving first and second G*â*teaux derivatives of the Lagrangian with respect to the state (i.e. displacements) and unknown viscoelastic material parameters. Though fragments of these viscoelasticity operators have been derived in previous works [1, 2, 3, 4, 5, 6, 7], in this report we present a derivation of the complete set of operators from first principles.

Once the optimization operators are defined, we derive the objective function, gradient and Hessian operations that are used to interface with the optimization solver. These methods have been implemented in the Sierra-SD framework [9, 10], leveraging much of the same infrastructure that was recently developed for force identification [11], as well as recent Helmholtz solver development to solve the frequency-domain equations resulting from the forward and adjoint problems. The objective function, gradient, and Hessian operations provide a natural interface to the Rapid Optimization Library (ROL), which is part of Trilinos [12]. Several methods from ROL have been tested for solving the viscoelastic inverse problem, and we present those results later in this report.

This report is organized as follows. First, we provide formulations for the forward problems of interest. Then, the inverse problem is cast in a PDE-constrained optimization framework. We derive the abstract optimization operators for viscoelasticity and provide precise details for the efficient computation of gradients and Hessians using an adjoint-based approach. We then then present results of a comparison of numerical results for the viscoelastic bulk and shear moduli of a foam block model, which was recently used in

experimental testing for foam property characterization.

2 Linear Viscoelasticity Formulation for Steady-State Dynamics

The equations of motion of a solid body in three dimensions are given by

$$\begin{aligned} -\omega^2 \rho \boldsymbol{u} - \nabla : \boldsymbol{\sigma} &= \boldsymbol{f}(\boldsymbol{x}, \omega) \quad \Omega \\ \boldsymbol{u}(\boldsymbol{x}, \omega) &= 0 \quad \boldsymbol{x} \in \Gamma_D \\ \boldsymbol{\sigma}(\boldsymbol{x}, \omega) \cdot \boldsymbol{n} &= \boldsymbol{t}(\boldsymbol{x}, \omega) \quad \boldsymbol{x} \in \Gamma_N \end{aligned} \tag{1}$$

where $\boldsymbol{u} = (u_1, u_2, u_3)$ is the complex vector of displacements, Ω is the domain of interest, $\boldsymbol{\sigma}$ is the stress tensor, $\boldsymbol{t}(\boldsymbol{x}, \omega)$ is a surface traction, and $\boldsymbol{f}(x,t)$ is the body force. The boundary of Ω is divided into Dirchlet Γ_D and Neumann Γ_N subregions.

The Dirichlet conditions lead to the space of admissible functions

$$V = \left[\boldsymbol{v} \in H^1(\Omega), \boldsymbol{v}(\boldsymbol{x}) = 0, \boldsymbol{x} \in \Gamma_D \right] \tag{2}$$

The equation of motion, along with boundary conditions, is cast into the weak form in the standard way. Find $\boldsymbol{u} \in V$

$$\int_\Omega \left[-\omega^2 \rho \boldsymbol{u} \cdot \bar{\boldsymbol{v}} + \boldsymbol{\sigma} : \nabla \bar{\boldsymbol{v}} \right] d\Omega = \int_\Omega \boldsymbol{f}(\boldsymbol{x}, \omega) \cdot \bar{\boldsymbol{v}} d\Omega + \int_{\Gamma_N} \boldsymbol{g}(\boldsymbol{x}, \omega) \cdot \bar{\boldsymbol{v}} d\Gamma_N \quad \forall v \in V \tag{3}$$

where an integration by parts has been carried out on the middle term, and the bar superscript denotes the complex conjugation.

We note that the term involving the gradient of the test function can be replaced by its symmetric counterpart, and thus equation 3 can be understood with $\boldsymbol{\sigma} : \nabla \bar{\boldsymbol{v}}$ replaced by $\boldsymbol{\sigma} : \nabla_s \bar{\boldsymbol{v}} = \boldsymbol{\sigma} : \varepsilon(\bar{v})$, where $\nabla_s \bar{\boldsymbol{v}} = \frac{1}{2} \left[(\nabla \bar{\boldsymbol{v}}) + (\nabla \bar{\boldsymbol{v}})^T \right]$, and $\boldsymbol{\varepsilon}(\boldsymbol{u}) = \nabla_s \boldsymbol{u} = \boldsymbol{B}\boldsymbol{u} = \frac{1}{2} \left[(\nabla \boldsymbol{u}) + (\nabla \boldsymbol{u})^T \right]$.

We now discuss some relations that will be useful for later derivations.

$$\begin{aligned} \boldsymbol{\varepsilon}_{ij} &= \frac{1}{3} \boldsymbol{\varepsilon}_{kk} \boldsymbol{\delta}_{ij} + \left(\boldsymbol{\varepsilon}_{ij} - \frac{1}{3} \boldsymbol{\varepsilon}_{kk} \boldsymbol{\delta}_{ij} \right) \\ &= \frac{1}{3} \boldsymbol{\varepsilon}^v_{ij} + \boldsymbol{\varepsilon}^d_{ij} \end{aligned} \tag{4}$$

Where $\boldsymbol{\varepsilon}^v_{ij} = \boldsymbol{\varepsilon}_{kk} \boldsymbol{\delta}_{ij}$ is the volumetric strain tensor and $\varepsilon^d_{ij} = \boldsymbol{\varepsilon}_{ij} - \frac{1}{3} \boldsymbol{\varepsilon}_{kk} \boldsymbol{\delta}_{ij}$ is the deviatoric strain tensor. That is, we can decompose the strain into volumetric and deviatoric components. Similarly, given the shear (G) and bulk (b) moduli, we can write the stress as

$$\boldsymbol{\sigma}_{ij} = b \boldsymbol{\varepsilon}^v_{ij} + 2G \boldsymbol{\varepsilon}^d_{ij} \tag{5}$$

In defining the constitutive model, it is often more convenient to work in terms of Voigt

notation where the stress and strain are defined in terms of vectors

$$\boldsymbol{\sigma} = \begin{bmatrix} \sigma_{xx} \\ \sigma_{yy} \\ \sigma_{zz} \\ \sigma_{yz} \\ \sigma_{xz} \\ \sigma_{xy} \end{bmatrix} \tag{6}$$

and

$$\boldsymbol{\varepsilon} = \begin{bmatrix} \varepsilon_{xx} \\ \varepsilon_{yy} \\ \varepsilon_{zz} \\ \varepsilon_{yz} \\ \varepsilon_{xz} \\ \varepsilon_{xy} \end{bmatrix} \tag{7}$$

With the Voigt notation, the constitutive equation for an elastic material can be written in terms of the shear and bulk moduli

$$\boldsymbol{\sigma} = \boldsymbol{D}\boldsymbol{\varepsilon} = (b\boldsymbol{D}_b + G\boldsymbol{D}_G)\boldsymbol{\varepsilon} \tag{8}$$

where $\boldsymbol{\sigma}$ and $\boldsymbol{\varepsilon}$ are understood in the Voigt (vector) format, and

$$\boldsymbol{D}_b = \begin{bmatrix} 1 & 1 & 1 & 0 & 0 & 0 \\ 1 & 1 & 1 & 0 & 0 & 0 \\ 1 & 1 & 1 & 0 & 0 & 0 \\ 0 & 0 & 0 & 0 & 0 & 0 \\ 0 & 0 & 0 & 0 & 0 & 0 \\ 0 & 0 & 0 & 0 & 0 & 0 \end{bmatrix} \tag{9}$$

and

$$\boldsymbol{D}_G = \begin{bmatrix} \frac{4}{3} & -\frac{2}{3} & -\frac{2}{3} & 0 & 0 & 0 \\ -\frac{2}{3} & \frac{4}{3} & -\frac{2}{3} & 0 & 0 & 0 \\ -\frac{2}{3} & -\frac{2}{3} & \frac{4}{3} & 0 & 0 & 0 \\ 0 & 0 & 0 & 1 & 0 & 0 \\ 0 & 0 & 0 & 0 & 1 & 0 \\ 0 & 0 & 0 & 0 & 0 & 1 \end{bmatrix} \tag{10}$$

We note the difference between the bulk modulus notation b used here, and the strain-displacement relationship $\boldsymbol{\varepsilon}(\boldsymbol{u}) = \boldsymbol{B}\boldsymbol{u}$. In the latter case we use bold-face notation for $\boldsymbol{B}$, and for the bulk modulus we use lower case b.

In terms of Voigt notation, a similar decomposition of stress into its volumetric and deviatoric components can be written as follows.

$$\begin{aligned} \boldsymbol{\sigma} = \boldsymbol{D}\boldsymbol{\varepsilon} &= (b\boldsymbol{D}_b + G\boldsymbol{D}_G)\boldsymbol{\varepsilon} \\ &= b\boldsymbol{\varepsilon}_v + 2G\boldsymbol{\varepsilon}_d \end{aligned} \tag{11}$$

These expressions coincide with the ones given earlier in terms of tensor notation in equation 5. That is, the first term of equation 8 extracts the volumetric stress, whereas the second extracts the deviatoric stress. For the remainder of this report, we will use Voigt notation for convenience.

2.0.1 Linear Viscoelastic Materials

In the case of a linear viscoelastic material, this constitutive relation can be generalized as follows

$$\boldsymbol{\sigma}(\omega) = \boldsymbol{D}(\omega)\boldsymbol{\varepsilon} = (b(\omega)\boldsymbol{D}_b + G(\omega)\boldsymbol{D}_G)\boldsymbol{\varepsilon}(\omega) \tag{12}$$

where the bulk and shear moduli $b(\omega)$ and $G(\omega)$ are complex-valued scalar functions of ω. Typically, these functions are broken into their real and imaginary parts

$$\begin{aligned} b(\omega) &= b_R(\omega) + ib_I(\omega) \\ G(\omega) &= G_R(\omega) + iG_I(\omega) \end{aligned} \tag{13}$$

where $b_R(\omega)$ and $G_R(\omega)$ are referred to as the *storage* moduli, and $b_I(\omega)$ and $G_I(\omega)$ are referred to as the *loss* moduli. Thus far, the moduli given here are independent of x. Later in this report we address the case where the moduli are spatially variable. The storage and loss moduli can be general functions of ω. A particular case would be a Prony series representation, but here we leave the expressions in the general form.

3 Inverse Problem Formulation

We will work with discretized PDEs and Euclidian spaces in these derivations. Our optimization problem will be abstractly defined as

$$\begin{aligned} \underset{\boldsymbol{u},\boldsymbol{p}}{\text{minimize}} \quad & J(\boldsymbol{u},\boldsymbol{p}) \\ \text{subject to} \quad & \boldsymbol{g}(\boldsymbol{u},\boldsymbol{p}) = \boldsymbol{0} \end{aligned}$$

where $\boldsymbol{u} \in \Re^n$ is the state vector, $\boldsymbol{p} \in \Re^m$ is the parameter vector, $J : \Re^n \times \Re^m \to \Re$ is the cost function and $\boldsymbol{g} : \Re^n \times \Re^m \to \Re^n$ represents the discretized constraint equations.

To derive the optimality conditions, we define a Lagrangian functional as

$$\mathscr{L}(\boldsymbol{u},\boldsymbol{p},\boldsymbol{w}) := J + \boldsymbol{w}^T \boldsymbol{g} \tag{14}$$

The first-order optimality conditions are given as

$$\begin{Bmatrix} \mathscr{L}_u \\ \mathscr{L}_p \\ \mathscr{L}_w \end{Bmatrix} = \begin{Bmatrix} J_u + \boldsymbol{g}_u^T \boldsymbol{w} \\ J_p + \boldsymbol{g}_p^T \boldsymbol{w} \\ \boldsymbol{g} \end{Bmatrix} = \{\boldsymbol{0}\} \tag{15}$$

where J_u is the derivative of the objective function with respect to the state variables, J_p is the derivative with respect to the design parameters, etc. A Newton iteration involves the following system

$$\begin{bmatrix} \mathscr{L}_{uu} & \mathscr{L}_{up} & \boldsymbol{g}_u^T \\ \mathscr{L}_{pu} & \mathscr{L}_{pp} & \boldsymbol{g}_p^T \\ \boldsymbol{g}_u & \boldsymbol{g}_p & \boldsymbol{0} \end{bmatrix} \begin{Bmatrix} \delta\boldsymbol{u} \\ \delta\boldsymbol{p} \\ \boldsymbol{w}^\star \end{Bmatrix} = - \begin{Bmatrix} J_u \\ J_p \\ \boldsymbol{g} \end{Bmatrix} \tag{16}$$

where $\boldsymbol{w}^\star = \boldsymbol{w} + \delta\boldsymbol{w}$ represents the updated quantity in a Newton iteration. The latter stems from the linearity of the system with respect to $\boldsymbol{w}$.

3.1 Complex-Valued Functions

In the case of complex valued functions, we take special care in defining some of the operations defined above. The state variables are split into real and imaginary parts of $\boldsymbol{u}$. The same interpretation holds for $\boldsymbol{p}$. That is, in the complex-valued case, $\boldsymbol{u} = [\boldsymbol{u}_R \ \boldsymbol{u}_I]$, $\boldsymbol{p} = [\boldsymbol{p}_R \ \boldsymbol{p}_I]$. The minimization is carried out with respect to real and imaginary parts independently. The general operations defined in the previous section for real-valued functions then carry forward naturally. We now highlight some points to be considered in the case of complex-valued functions. The real and imaginary components of the constraint equations are enforced separately. That is, the Lagrangian is given as

$$\mathscr{L}(\boldsymbol{u},\boldsymbol{p},\boldsymbol{w}) := J + \boldsymbol{w}_R^T \boldsymbol{g}_R + \boldsymbol{w}_I^T \boldsymbol{g}_I \tag{17}$$

$$= J + \Re(\boldsymbol{w}^H \boldsymbol{g}) \text{ (short-hand representation)} \tag{18}$$

where $\Re(\boldsymbol{a})$ denotes the real part of $\boldsymbol{a}$, and $\boldsymbol{w}^H$ is the hermitian transpose. Also, the subindexes R and I denote the real and imaginary parts of a quantity. Now, since we are treating real and imaginary parts as independent variables in the optimization problem, derivatives of real-valued functions with respect to complex-valued functions are interpreted as $\mathscr{L}_u = [\mathscr{L}_{u_R}\ \mathscr{L}_{u_I}]$, $J_u = [J_{u_R}\ J_{u_I}]$, etc. The derivatives of complex-valued functions will be interpreted as,

$$\boldsymbol{g}_u^T = \begin{bmatrix} \boldsymbol{g}_{R_{u_R}}^T & \boldsymbol{g}_{I_{u_R}}^T \\ \boldsymbol{g}_{R_{u_I}}^T & \boldsymbol{g}_{I_{u_I}}^T \end{bmatrix},\ \boldsymbol{g}_p^T = \begin{bmatrix} \boldsymbol{g}_{R_{p_R}}^T & \boldsymbol{g}_{I_{p_R}}^T \\ \boldsymbol{g}_{R_{p_I}}^T & \boldsymbol{g}_{I_{p_I}}^T \end{bmatrix},\ \text{etc.}$$

3.2 Reduced-space Newton

This approach is equivalent to solving an unconstrained optimization problem in the space of parameters only. To this end, we will use the objective function $\hat{J}(\boldsymbol{p}) = J(\boldsymbol{u}(\boldsymbol{p}), \boldsymbol{p})$. The steps involved in the reduced-space Newton approach are

1. Computing the state vector $\boldsymbol{u}$ from the forward problem

$$\boldsymbol{g} = \boldsymbol{0}, \tag{19}$$

   which corresponds to the elimination of the third equation in (15).

2. Computing the adjoint vector $\boldsymbol{w}$ by solving

$$\boldsymbol{g}_u^T \boldsymbol{w} = -J_u, \tag{20}$$

   which corresponds to eliminating the first equation in (15).

3. Evaluating the (reduced) gradient of the objective function with respect to the design vector as

$$\hat{J}' = J_p + \boldsymbol{g}_p^T \boldsymbol{w} \tag{21}$$

4. Evaluating the objective function

$$\hat{J}(\boldsymbol{p}) \tag{22}$$

5. Solving the Newton step problem

$$\boldsymbol{W}\Delta\boldsymbol{p} = -\hat{J}', \tag{23}$$

   where the reduced Hessian $\boldsymbol{W}$ can be obtained as the Schur complement of $\mathscr{L}_{pp}$ from (16) and is given as

$$\boldsymbol{W} = \boldsymbol{g}_p^T \boldsymbol{g}_u^{-T} (\mathscr{L}_{uu} \boldsymbol{g}_u^{-1} \boldsymbol{g}_p - \mathscr{L}_{up}) - \mathscr{L}_{pu} \boldsymbol{g}_u^{-1} \boldsymbol{g}_p + \mathscr{L}_{pp} \tag{24}$$

The evaluation of the action of the reduced-hessian on a vector $\boldsymbol{s}$, e.g. $\boldsymbol{W}\boldsymbol{s}$, is obtained as follows

1. Compute (forward problem)
$$\boldsymbol{h}_1 = \boldsymbol{g}_u^{-1}\boldsymbol{g}_p\boldsymbol{s} \tag{25}$$

2. Compute
$$\boldsymbol{h}_2 = \mathscr{L}_{uu}\boldsymbol{h}_1 - \mathscr{L}_{up}\boldsymbol{s} \tag{26}$$

3. Compute (adjoint problem)
$$\boldsymbol{h}_3 = \boldsymbol{g}_u^{-T}\boldsymbol{h}_2 \tag{27}$$

4. Finally, compute
$$\boldsymbol{W}\boldsymbol{s} = \boldsymbol{g}_p^T\boldsymbol{h}_3 - \mathscr{L}_{pu}\boldsymbol{h}_1 + \mathscr{L}_{pp}\boldsymbol{s} \tag{28}$$

3.3 Derivation of Abstract Optimization Operators

Given a finite dimensional subspace $V_h \subset V$, we represent the approximate solution in the standard way
$$\boldsymbol{u}_h(\boldsymbol{x},\omega) = \sum_{i=1}^{n} \boldsymbol{u}_i(\omega)\phi_i(\boldsymbol{x}) \tag{29}$$

where $V_h = span(\phi_i)$, and $\boldsymbol{u}_i(\omega)$ represent the unknown frequency-dependent coefficients. We also denote $\boldsymbol{\Phi}(x) = [\phi_i(x)]$ as the matrix having ϕ_i as the i^{th} column. Inserting this into the weak form 3, and rearranging, we obtain

$$\boldsymbol{K}\boldsymbol{u} - \omega^2\boldsymbol{M}\boldsymbol{u} = \boldsymbol{f} \tag{30}$$

where

$$\begin{aligned}
\boldsymbol{K} &= \int_\Omega \boldsymbol{B}^T\boldsymbol{D}\boldsymbol{B}d\Omega \\
&= \int_\Omega \boldsymbol{B}^T(b\boldsymbol{D}_b + G\boldsymbol{D}_G)\boldsymbol{B}d\Omega \\
&= \int_\Omega \boldsymbol{B}^T(\Re(b)\boldsymbol{D}_b + \Re(G)\boldsymbol{D}_G)\boldsymbol{B}d\Omega \\
&+ i\int_\Omega \boldsymbol{B}^T(\Im(b)\boldsymbol{D}_b + \Im(G)\boldsymbol{D}_G)\boldsymbol{B}d\Omega \\
&= \boldsymbol{K}_R + i\boldsymbol{K}_I,
\end{aligned} \tag{31}$$

and
$$\boldsymbol{M} = \int_\Omega \rho\boldsymbol{\Phi}\boldsymbol{\Phi}^T d\Omega \tag{32}$$

Next, we wish to compute the action of the derivatives $\boldsymbol{g}^T$ on the adjoint solution $\boldsymbol{w}$, as required in equation 21.

$$\mathscr{L}_p = \begin{bmatrix}\mathscr{L}_{p_R}\\ \mathscr{L}_{p_I}\end{bmatrix} = \begin{bmatrix}J_{p_R}\\ J_{p_I}\end{bmatrix} + \begin{bmatrix}\boldsymbol{g}_{R_{p_R}}^T & \boldsymbol{g}_{I_{p_R}}^T\\ \boldsymbol{g}_{R_{p_I}}^T & \boldsymbol{g}_{I_{p_I}}^T\end{bmatrix}\begin{bmatrix}\boldsymbol{w}_R\\ \boldsymbol{w}_I\end{bmatrix} \tag{33}$$

We can write the real and imaginary parts of the $\boldsymbol{g}$ operator in terms of the stiffness and mass matrices as follows. First, we note that the stiffness matrix $\boldsymbol{K} = \boldsymbol{K}_R + i\boldsymbol{K}_I$ and solution vector $\boldsymbol{u} = \boldsymbol{u}_R + i\boldsymbol{u}_I$ can be split into real and imaginary parts. Then, we have the following decomposition

$$\begin{aligned} \boldsymbol{g}_R^T &= \left(\boldsymbol{K}_R\boldsymbol{u}_R - \boldsymbol{K}_I\boldsymbol{u}_I - \omega^2\boldsymbol{M}\boldsymbol{u}_R - \boldsymbol{f}_R\right)^T \\ &= \boldsymbol{u}_R^T\boldsymbol{K}_R - \boldsymbol{u}_I^T\boldsymbol{K}_I - \omega^2\boldsymbol{u}_R^T\boldsymbol{M} - f_R^T \\ \boldsymbol{g}_I^T &= \left(\boldsymbol{K}_R\boldsymbol{u}_I + \boldsymbol{K}_I\boldsymbol{u}_R - \omega^2\boldsymbol{M}\boldsymbol{u}_I - \boldsymbol{f}_I\right)^T \\ &= \boldsymbol{u}_I^T\boldsymbol{K}_R + \boldsymbol{u}_R^T\boldsymbol{K}_I - \omega^2\boldsymbol{u}_I^T\boldsymbol{M} - \boldsymbol{f}_I^T \end{aligned} \tag{34}$$

Here we restrict ourselves to symmetric stiffness and mass matrices.

In deriving the derivatives with respect to parameters, we consider a single frequency ω, since the solutions at each frequency are independent of one another. For the parameters $G_R = \Re(G)$, $G_I = \Im(G)$, $b_R = \Re(b)$, $b_I = \Im(b)$, the derivatives are straightforward. We consider two subcases, first where the parameters are constant over the domain Ω, and second where they vary element-by-element. In the case where they are constant, and taking the bulk modulus as an example, we have

$$\boldsymbol{g}_{R,b_R}^T = \int_\Omega \boldsymbol{u}_R^T\boldsymbol{B}^T\boldsymbol{D}_b\boldsymbol{B}d\Omega = \sum_e \int_{\Omega_e} \boldsymbol{u}_R^T\boldsymbol{B}^T\boldsymbol{D}_b\boldsymbol{B}d\Omega_e \tag{35}$$

where we break the above integral into element-wise contributions, and $\Omega = \sum_e \Omega_e$, where Ω_e corresponds to the volume of an individual finite element. In the second case, we consider the scenario where the parameters are piecewise constant over the elements. Here the derivatives with respect to one of the element parameters reduce to the integral over the modulus parameter for that given element, since the other element contributions have no contribution from the given parameter. Thus, again considering the bulk modulus as an example we have

$$\boldsymbol{g}_{R,b_R}^T = \int_{\Omega_e} \boldsymbol{u}_R^T\boldsymbol{B}^T\boldsymbol{D}_b\boldsymbol{B}d\Omega_e \tag{36}$$

where in this case the entire integral collapses to an integral over the element that contains the parameter of interest. From now on, to simplify notation, we will consider the derivatives over a single element, since that is the building block for all cases.

Taking derivatives over each element separately, we have

$$\begin{aligned} \boldsymbol{g}_{R,b_R}^T\boldsymbol{w}_R &= \int_{\Omega_e} \boldsymbol{u}_R^T\boldsymbol{B}^T\boldsymbol{D}_b\boldsymbol{B}\boldsymbol{w}_R d\Omega_e \\ &= \int_{\Omega_e} \boldsymbol{\varepsilon}(\boldsymbol{u}_R)^T\boldsymbol{\varepsilon}_v(\boldsymbol{w}_R)d\Omega_e \\ &= \int_{\Omega_e} \boldsymbol{\varepsilon}_v(\boldsymbol{u}_R)^T\boldsymbol{\varepsilon}_v(\boldsymbol{w}_R)d\Omega_e \end{aligned} \tag{37}$$

Similarly, for the real part of the shear modulus we have

$$\begin{aligned} \boldsymbol{g}_{R,G_R}^T \boldsymbol{w}_R &= 2\int_{\Omega_e} \boldsymbol{u}_R^T \boldsymbol{B}^T \boldsymbol{D}_G \boldsymbol{B} \boldsymbol{w}_R d\Omega_e \\ &= 2\int_{\Omega_e} \boldsymbol{\varepsilon}(\boldsymbol{u}_R)^T \boldsymbol{\varepsilon}_d(\boldsymbol{w}_R) d\Omega_e \\ &= 2\int_{\Omega_e} \boldsymbol{\varepsilon}_d(\boldsymbol{u}_R)^T \boldsymbol{\varepsilon}_d(\boldsymbol{w}_R) d\Omega_e \end{aligned} \tag{38}$$

The remaining expressions are as follows

$$\begin{aligned} \boldsymbol{g}_{R,b_I}^T \boldsymbol{w}_R &= -\int_{\Omega_e} \boldsymbol{\varepsilon}_v(\boldsymbol{u}_I)^T \boldsymbol{\varepsilon}_v(\boldsymbol{w}_R) d\Omega_e \\ \boldsymbol{g}_{R,G_I}^T \boldsymbol{w}_R &= -2\int_{\Omega_e} \boldsymbol{\varepsilon}_d(\boldsymbol{u}_I)^T \boldsymbol{\varepsilon}_d(\boldsymbol{w}_R) d\Omega_e \\ \boldsymbol{g}_{I,b_R}^T \boldsymbol{w}_I &= \int_{\Omega_e} \boldsymbol{\varepsilon}_v(\boldsymbol{u}_I)^T \boldsymbol{\varepsilon}_v(\boldsymbol{w}_I) d\Omega_e \\ \boldsymbol{g}_{I,b_I}^T \boldsymbol{w}_I &= \int_{\Omega_e} \boldsymbol{\varepsilon}_v(\boldsymbol{u}_R)^T \boldsymbol{\varepsilon}_v(\boldsymbol{w}_I) d\Omega_e \\ \boldsymbol{g}_{I,G_R}^T \boldsymbol{w}_I &= 2\int_{\Omega_e} \boldsymbol{\varepsilon}_d(\boldsymbol{u}_I)^T \boldsymbol{\varepsilon}_d(\boldsymbol{w}_I) d\Omega_e \\ \boldsymbol{g}_{I,G_I}^T \boldsymbol{w}_I &= 2\int_{\Omega_e} \boldsymbol{\varepsilon}_d(\boldsymbol{u}_R)^T \boldsymbol{\varepsilon}_d(\boldsymbol{w}_I) d\Omega_e \end{aligned} \tag{39}$$

Finally, if we consider the case of only a single element and a single unknown material, we would have four unknown parameters, b_R, G_R, b_I, G_I. In that case we can combine the above expressions

$$\begin{bmatrix} \boldsymbol{g}_{R_{p_R}}^T & \boldsymbol{g}_{I_{p_R}}^T \\ \boldsymbol{g}_{R_{p_I}}^T & \boldsymbol{g}_{I_{p_I}}^T \end{bmatrix} \begin{bmatrix} \boldsymbol{w}_R \\ \boldsymbol{w}_I \end{bmatrix} = \begin{bmatrix} \int_{\Omega_e} \boldsymbol{\varepsilon}_v(\boldsymbol{u}_R)^T \boldsymbol{\varepsilon}_v(\boldsymbol{w}_R) + \boldsymbol{\varepsilon}_v(\boldsymbol{u}_I)^T \boldsymbol{\varepsilon}_v(\boldsymbol{w}_I) d\Omega_e \\ 2\int_{\Omega_e} \boldsymbol{\varepsilon}_d(\boldsymbol{u}_R)^T \boldsymbol{\varepsilon}_d(\boldsymbol{w}_R) + \boldsymbol{\varepsilon}_d(\boldsymbol{u}_I)^T \boldsymbol{\varepsilon}_d(\boldsymbol{w}_I) d\Omega_e \\ \int_{\Omega_e} \boldsymbol{\varepsilon}_v(\boldsymbol{u}_R)^T \boldsymbol{\varepsilon}_v(\boldsymbol{w}_I) - \boldsymbol{\varepsilon}_v(\boldsymbol{u}_I)^T \boldsymbol{\varepsilon}_v(\boldsymbol{w}_R) d\Omega_e \\ 2\int_{\Omega_e} \boldsymbol{\varepsilon}_d(\boldsymbol{u}_R)^T \boldsymbol{\varepsilon}_d(\boldsymbol{w}_I) - \varepsilon_d(\boldsymbol{u}_I)^T \boldsymbol{\varepsilon}_d(\boldsymbol{w}_R) d\Omega_e \end{bmatrix} \tag{40}$$

In summary, equation 40 defines the gradient contribution to the parameters over a single element. If the parameters are constant over the domain, then there would be an additional element-level summation over the domain Ω to complete the calculation of the gradient.

We see from equation 24 that the remaining operators that need to be evaluated for viscoelastic materials are $\mathscr{L}_{pu}$, $\mathscr{L}_{pp}$, and $\mathscr{L}_{up}$. It is easy to see that $\mathscr{L}_{pp} = 0$, since the right hand side of equation 40 does not depend on the parameters. Also, we note that the mixed derivatives of the objective function $J_{up} = J_{pu} = 0$ are zero, since the state and design variables are involved in separate terms in the objective function. We need to evaluate the action of $\mathscr{L}_{pu}$ on a vector $\boldsymbol{h}_1$, as given in equation 25. This proceeds as follows

$$\mathscr{L}_{pu} \boldsymbol{h}_1 = \begin{bmatrix} \mathscr{L}_{p_R u_R} & \mathscr{L}_{p_R u_I} \\ \mathscr{L}_{p_I u_R} & \mathscr{L}_{p_I u_I} \end{bmatrix} \begin{bmatrix} \boldsymbol{h}_{1R} \\ \boldsymbol{h}_{1I} \end{bmatrix} \tag{41}$$

Since $J_{pu} = 0$, each component of the proceeding matrix can be computed as

$$\begin{aligned}
\mathscr{L}_{p_R u_R} &= \boldsymbol{g}^T_{R,p_R u_R} \boldsymbol{w}_R + \boldsymbol{g}^T_{I,p_R u_R} \boldsymbol{w}_I \\
\mathscr{L}_{p_R u_I} &= \boldsymbol{g}^T_{R,p_R u_I} \boldsymbol{w}_R + \boldsymbol{g}^T_{I,p_R u_I} \boldsymbol{w}_I \\
\mathscr{L}_{p_I u_R} &= \boldsymbol{g}^T_{R,p_I u_R} \boldsymbol{w}_R + \boldsymbol{g}^T_{I,p_I u_R} \boldsymbol{w}_I \\
\mathscr{L}_{p_I u_I} &= \boldsymbol{g}^T_{R,p_I u_I} \boldsymbol{w}_R + \boldsymbol{g}^T_{I,p_I u_I} \boldsymbol{w}_I
\end{aligned} \tag{42}$$

Recalling equation 34, we see that several of the terms are zero

$$\boldsymbol{g}^T_{R,p_R u_I} = \boldsymbol{g}^T_{R,p_I u_R} = \boldsymbol{g}^T_{I,p_R u_R} = \boldsymbol{g}^T_{I,p_I u_I} = 0 \tag{43}$$

which implies that

$$\begin{aligned}
\mathscr{L}_{p_R u_R} &= \boldsymbol{g}^T_{R,p_R u_R} \boldsymbol{w}_R \\
\mathscr{L}_{p_R u_I} &= \boldsymbol{g}^T_{I,p_R u_I} \boldsymbol{w}_I \\
\mathscr{L}_{p_I u_R} &= \boldsymbol{g}^T_{I,p_I u_R} \boldsymbol{w}_I \\
\mathscr{L}_{p_I u_I} &= \boldsymbol{g}^T_{R,p_I u_I} \boldsymbol{w}_R
\end{aligned} \tag{44}$$

Next we evaluate the remaining derivatives in a similar way as was done for the gradient. We note that terms like $\boldsymbol{g}^T_{R,p_R u_R} \boldsymbol{w}_R$ will actually be acting on a perterbation vector $\boldsymbol{h}_1$ as per equation 28, and thus we have for the real part of the $\boldsymbol{g}^T$ operator

$$\begin{aligned}
(\boldsymbol{g}^T_{R,b_R u_R} \boldsymbol{w}_R) \boldsymbol{h}_{1R} = \boldsymbol{h}^T_{1R} \boldsymbol{g}^T_{R,b_R u_R} \boldsymbol{w}_R &= \int_{\Omega_e} \boldsymbol{\varepsilon}_v(\boldsymbol{h}_{1R})^T \boldsymbol{\varepsilon}_v(\boldsymbol{w}_R) d\Omega_e \\
(\boldsymbol{g}^T_{R,G_R u_R} \boldsymbol{w}_R) \boldsymbol{h}_{1R} &= 2 \int_{\Omega_e} \boldsymbol{\varepsilon}_d(\boldsymbol{h}_{1R})^T \boldsymbol{\varepsilon}_d(\boldsymbol{w}_R) d\Omega_e \\
(g^T_{I,b_I u_R} \boldsymbol{w}_I) \boldsymbol{h}_{1R} &= \int_{\Omega_e} \boldsymbol{\varepsilon}_v(\boldsymbol{h}_{1R})^T \boldsymbol{\varepsilon}_v(\boldsymbol{w}_I) d\Omega_e \\
(g^T_{I,G_I u_R} \boldsymbol{w}_I) \boldsymbol{h}_{1R} &= 2 \int_{\Omega_e} \boldsymbol{\varepsilon}_d(\boldsymbol{h}_{1R})^T \boldsymbol{\varepsilon}_d(\boldsymbol{w}_I) d\Omega_e
\end{aligned} \tag{45}$$

and the following expressions for the imaginary part of $\boldsymbol{h}_1$

$$\begin{aligned}
(g^T_{R,b_I u_I} \boldsymbol{w}_R) \boldsymbol{h}_{1I} &= -\int_{\Omega_e} \boldsymbol{\varepsilon}_v(\boldsymbol{h}_{1I})^T \boldsymbol{\varepsilon}_v(\boldsymbol{w}_R) d\Omega_e \\
(\boldsymbol{g}^T_{R,G_I u_I} \boldsymbol{w}_R) \boldsymbol{h}_{1I} &= -2 \int_{\Omega_e} \boldsymbol{\varepsilon}_d(\boldsymbol{h}_{1I})^T \boldsymbol{\varepsilon}_d(\boldsymbol{w}_R) d\Omega_e \\
(g^T_{I,b_R u_I} \boldsymbol{w}_I) \boldsymbol{h}_{1I} &= \int_{\Omega_e} \boldsymbol{\varepsilon}_v(\boldsymbol{h}_{1I})^T \boldsymbol{\varepsilon}_v(\boldsymbol{w}_I) d\Omega_e \\
(g^T_{I,G_R u_I} \boldsymbol{w}_I) \boldsymbol{h}_{1I} &= 2 \int_{\Omega_e} \boldsymbol{\varepsilon}_d(\boldsymbol{h}_{1I})^T \boldsymbol{\varepsilon}_d(\boldsymbol{w}_I) d\Omega_e
\end{aligned} \tag{46}$$

Finally, we have

$$\mathscr{L}_{pu} \boldsymbol{h}_1 = \begin{bmatrix} \mathscr{L}_{p_R u_R} & \mathscr{L}_{p_R u_I} \\ \mathscr{L}_{p_I u_R} & \mathscr{L}_{p_I u_I} \end{bmatrix} \begin{bmatrix} \boldsymbol{h}_{1R} \\ \boldsymbol{h}_{1I} \end{bmatrix} = \begin{bmatrix} \int_{\Omega_e} \boldsymbol{\varepsilon}_v(\boldsymbol{h}_{1R})^T \boldsymbol{\varepsilon}_v(\boldsymbol{w}_R) d\Omega_e + \boldsymbol{\varepsilon}_v(\boldsymbol{h}_{1I})^T \boldsymbol{\varepsilon}_v(\boldsymbol{w}_I) d\Omega_e \\ \int_{\Omega_e} 2\boldsymbol{\varepsilon}_d(\boldsymbol{h}_{1R})^T \boldsymbol{\varepsilon}_d(\boldsymbol{w}_R) + 2\boldsymbol{\varepsilon}_d(\boldsymbol{h}_{1I})^T \boldsymbol{\varepsilon}_d(\boldsymbol{w}_I) d\Omega_e \\ \int_{\Omega_e} \boldsymbol{\varepsilon}_v(\boldsymbol{h}_{1R})^T \boldsymbol{\varepsilon}_v(\boldsymbol{w}_I) - \boldsymbol{\varepsilon}_v(\boldsymbol{h}_{1I})^T \boldsymbol{\varepsilon}_v(\boldsymbol{w}_R) d\Omega_e \\ \int_{\Omega_e} 2\boldsymbol{\varepsilon}_d(\boldsymbol{h}_{1R})^T \boldsymbol{\varepsilon}_d(\boldsymbol{w}_I) - 2\boldsymbol{\varepsilon}_d(\boldsymbol{h}_{1I})^T \boldsymbol{\varepsilon}_d(\boldsymbol{w}_R) d\Omega_e \end{bmatrix} \tag{47}$$

Next, we study the action of $\boldsymbol{g}_p$ on a perturbation vector s, as required from equation 25. We see that we will need the derivatives of both $\boldsymbol{g}_R$ and $\boldsymbol{g}_I$ with respect to both real and imaginary parts of the parameters. First, we write the PDE operators as

$$\begin{aligned} \boldsymbol{g}_R &= \boldsymbol{K}_R\boldsymbol{u}_R - \boldsymbol{K}_I\boldsymbol{u}_I - \omega^2\boldsymbol{M}\boldsymbol{u}_R - \boldsymbol{f}_R \\ \boldsymbol{g}_I &= \boldsymbol{K}_R\boldsymbol{u}_I + \boldsymbol{K}_I\boldsymbol{u}_R - \omega^2\boldsymbol{M}\boldsymbol{u}_I - \boldsymbol{f}_I \end{aligned} \tag{48}$$

Thus, we have

$$\begin{bmatrix} \boldsymbol{g}_{R,p_R} & \boldsymbol{g}_{R,p_I} \\ \boldsymbol{g}_{I,p_R} & \boldsymbol{g}_{I,p_I} \end{bmatrix} \begin{bmatrix} \boldsymbol{s}_R \\ \boldsymbol{s}_I \end{bmatrix} = \begin{bmatrix} \boldsymbol{K}_R(s_R)\boldsymbol{u}_R - \boldsymbol{K}_I(s_I)\boldsymbol{u}_I \\ \boldsymbol{K}_R(s_R)\boldsymbol{u}_I + \boldsymbol{K}_I(s_I)\boldsymbol{u}_R \end{bmatrix} \tag{49}$$

Where the notation $\boldsymbol{K}_R(s_R)$ indicates the real part of the stiffness matrix evaluated using the real part of the perturbation vector s_R as the parameter in the stiffness matrix evaluation. Similar interpretations hold for the other operators. Thus, action of $\boldsymbol{g}_p$ acting on a perturbation vector $\boldsymbol{s} = (\boldsymbol{s}_R, \boldsymbol{s}_I)$ is precisely given by equations 49, but where the stiffness matrices $\boldsymbol{K}_R$ and $\boldsymbol{K}_I$ are reassembled using the parameter vector $\boldsymbol{s} = (\boldsymbol{s}_R, \boldsymbol{s}_I)$.

Following a similar reasoning as for $\mathscr{L}_{pu}$, for $\mathscr{L}_{up}$ we have

$$\mathscr{L}_{up}\boldsymbol{s} = \begin{bmatrix} \mathscr{L}_{u_Rp_R} & \mathscr{L}_{u_Rp_I} \\ \mathscr{L}_{u_Ip_R} & \mathscr{L}_{u_Ip_I} \end{bmatrix} \begin{bmatrix} \boldsymbol{s}_R \\ \boldsymbol{s}_I \end{bmatrix} \tag{50}$$

where we note that now the 2×2 matrix operates directly on the perterbation vector $\boldsymbol{s}$, as given in equation 24. Since $J_{up} = 0$, each component of the proceeding matrix can be computed as

$$\begin{aligned} \mathscr{L}_{u_Rp_R} &= \boldsymbol{g}^T_{R,u_Rp_R}\boldsymbol{w}_R + \boldsymbol{g}^T_{I,u_Rp_R}\boldsymbol{w}_I \\ \mathscr{L}_{u_Rp_I} &= \boldsymbol{g}^T_{R,u_Rp_I}\boldsymbol{w}_R + \boldsymbol{g}^T_{I,u_Rp_I}\boldsymbol{w}_I \\ \mathscr{L}_{u_Ip_R} &= \boldsymbol{g}^T_{R,u_Ip_R}\boldsymbol{w}_R + \boldsymbol{g}^T_{I,u_Ip_R}\boldsymbol{w}_I \\ \mathscr{L}_{u_Ip_I} &= \boldsymbol{g}^T_{R,u_Ip_I}\boldsymbol{w}_R + \boldsymbol{g}^T_{I,u_Ip_I}\boldsymbol{w}_I \end{aligned} \tag{51}$$

When considering equation 34, we have the following observations

$$\boldsymbol{g}^T_{R,u_Rp_I} = \boldsymbol{g}^T_{R,u_Ip_R} = \boldsymbol{g}^T_{I,u_Rp_R} = \boldsymbol{g}^T_{I,u_Ip_I} = 0 \tag{52}$$

Thus, we have the following simplification

$$\begin{aligned} \mathscr{L}_{u_Rp_R} &= \boldsymbol{g}^T_{R,u_Rp_R}\boldsymbol{w}_R \\ \mathscr{L}_{u_Rp_I} &= \boldsymbol{g}^T_{I,u_Rp_I}\boldsymbol{w}_I \\ \mathscr{L}_{u_Ip_R} &= \boldsymbol{g}^T_{I,u_Ip_R}\boldsymbol{w}_I \\ \mathscr{L}_{u_Ip_I} &= \boldsymbol{g}^T_{R,u_Ip_I}\boldsymbol{w}_R \end{aligned} \tag{53}$$

$$
\begin{aligned}
\boldsymbol{g}_R^T &= \left(\boldsymbol{K}_R\boldsymbol{u}_R - \boldsymbol{K}_I\boldsymbol{u}_I - \omega^2\boldsymbol{M}\boldsymbol{u}_R - \boldsymbol{f}_R\right)^T \\
&= \boldsymbol{u}_R^T\boldsymbol{K}_R - \boldsymbol{u}_I^T\boldsymbol{K}_I - \omega^2\boldsymbol{u}_R^T\boldsymbol{M} - f_R^T \\
\boldsymbol{g}_I^T &= \left(\boldsymbol{K}_R\boldsymbol{u}_I + \boldsymbol{K}_I\boldsymbol{u}_R - \omega^2\boldsymbol{M}\boldsymbol{u}_I - \boldsymbol{f}_I\right)^T \\
&= \boldsymbol{u}_I^T\boldsymbol{K}_R + \boldsymbol{u}_R^T\boldsymbol{K}_I - \omega^2\boldsymbol{u}_I^T\boldsymbol{M} - \boldsymbol{f}_I^T
\end{aligned}
\tag{54}
$$

As seen from equation 24, the operator $\mathscr{L}_{up}$ will act on a perturbation vector in the design variables, $\boldsymbol{s} = (\boldsymbol{s}_R, \boldsymbol{s}_I)$. Thus, we have

$$
\begin{aligned}
\begin{bmatrix} \mathscr{L}_{u_Rp_R} & \mathscr{L}_{u_Rp_I} \\ \mathscr{L}_{u_Ip_R} & \mathscr{L}_{u_Ip_I} \end{bmatrix} \begin{bmatrix} \boldsymbol{s}_R \\ \boldsymbol{s}_I \end{bmatrix} &= \begin{bmatrix} \boldsymbol{g}_{R,u_Rp_R}^T\boldsymbol{w}_R & \boldsymbol{g}_{I,u_Rp_I}^T\boldsymbol{w}_I \\ \boldsymbol{g}_{I,u_Ip_R}^T\boldsymbol{w}_I & \boldsymbol{g}_{R,u_Ip_I}^T\boldsymbol{w}_R \end{bmatrix} \begin{bmatrix} \boldsymbol{s}_R \\ \boldsymbol{s}_I \end{bmatrix} \\
&= \begin{bmatrix} \boldsymbol{K}_R(s_R)\boldsymbol{w}_R + \boldsymbol{K}_I(s_I)\boldsymbol{w}_I \\ \boldsymbol{K}_R(s_R)\boldsymbol{w}_I - \boldsymbol{K}_I(s_I)\boldsymbol{w}_R \end{bmatrix}
\end{aligned}
\tag{55}
$$

4 Numerical Results on a Foam Block Model

In this section we describe results obtained on a foamblock model, as shown in Figure 1. Recent experiments have been conducted on this model involving hammer impact on one end, and corresponding accelerometer measurements as shown in Figure 1. Steel blocks on either end are joined by a foamblock consisting of a viscoelastic material. It is desired to compute the frequency-dependent real and imaginary components of bulk and shear modulus directly from the accelerometer measurements.

Before addressing the inverse problem, we performed a sensitivity analysis on the model. These results are shown in Figure 2, and show the percent change in acceleration as a function of frequency that results from a 20 percent change in the corresponding (real or imaginary) modulus. As expected, these curves show peaks that correspond to resonance modes of the structure. As the modes change differently with each parameter, the locations of the peaks are different for each change in the moduli. The locations of these peaks give an indication of the ideal frequencies for the inverse problem, as they correspond to maximum sensitivity.

The locations of the peaks do not coincide for the different material parameter changes, as shown in Figure 2, since the modes change differently with each parameter. Nonetheless, we selected a frequency of 500Hz for the inverse problem. Results at other frequencies that were near the sensitivity peaks showed similar results. Synthetic data was generated by running a forward problem with inputs at the location of the hammer impact, node 357 (see Figure 1), and recording the response at node 212. This data was then given as input to the inverse problem.

Table 1 shows the exact material properties at 500Hz, the initial guess, and the parameters predicted by the inverse problem. As shown, despite a very poor initial guess of assuming zero damping and a 50 percent drop in real moduli, the inverse problem recovers both the real and imaginary moduli remarkably well.

Figure 3 shows the convergence behaviour of Newton-trustregion and BFGS algorithms from ROL on this problem. The gradient and objective function both drop appreciably in 50 iterations. The Newton method converges more rapidly per iteration, though each iteration is more expensive than BFGS.

In this report we only present inverse results using synthetic data, that is, data that is generated by running a forward problem on the finite element mesh of the model. Experimental data is available for this model, and thus a study of the inverse problem with actual accelerometer data is underway and will be documented in a future report.

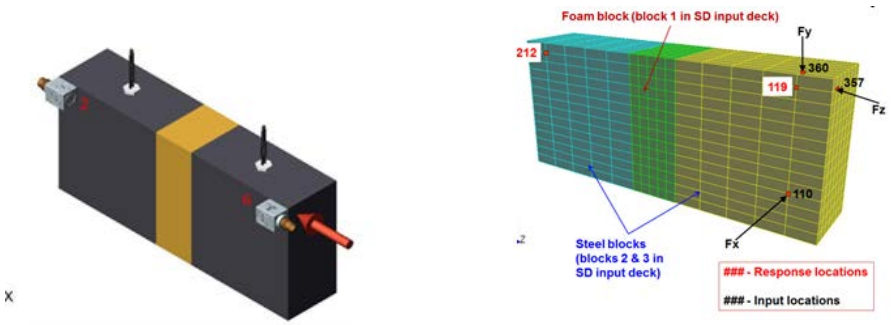

Picture of foamblock structure Finite element mesh of foamblock structure

Figure 1. The foam block model for viscoelastic material inversion studies.

Table 1. Results of foam block material inversion

Parameter	Exact	Initial Guess	Computed
Real part of K	40000	20000	40000.0013
Imag part of K	0	0	−0.00617
Real part of G	16000	8000	15999.99937
Imag part of G	5000	0	5000.000945

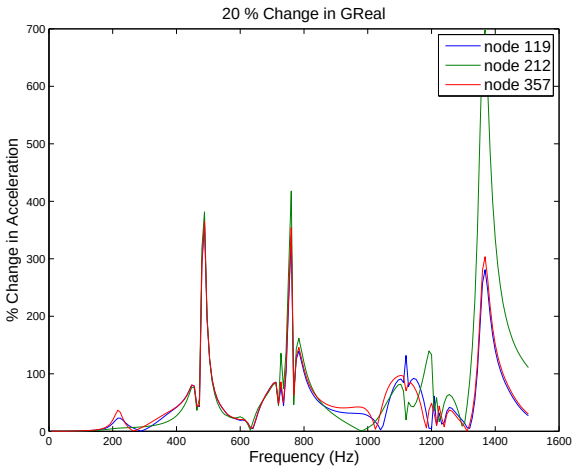

Sensitivity of solution to GReal.

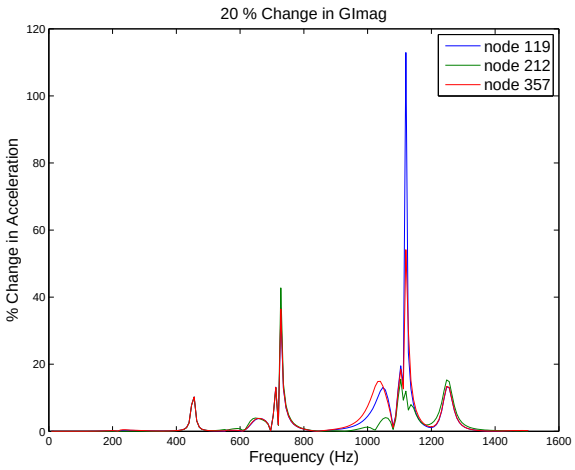

Sensitivity of solution to GImag.

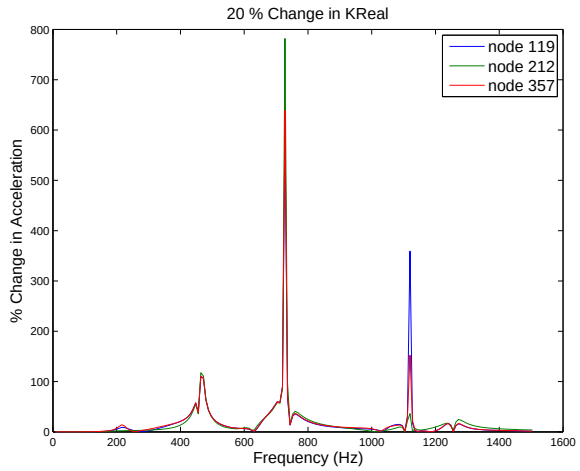

Sensitivity of solution to KReal.

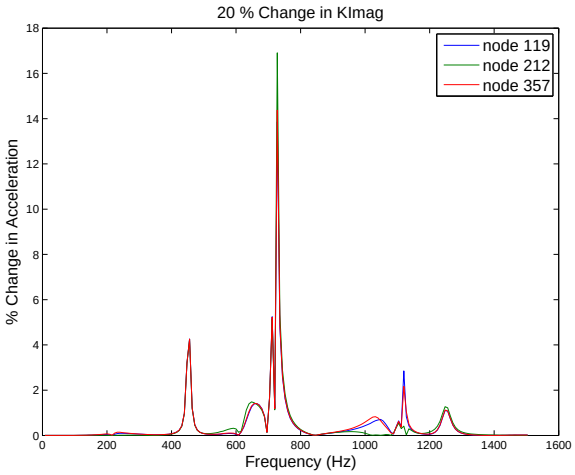

Sensitivity of solution to KImag.

Figure 2. Sensitivity analysis of foam block model.

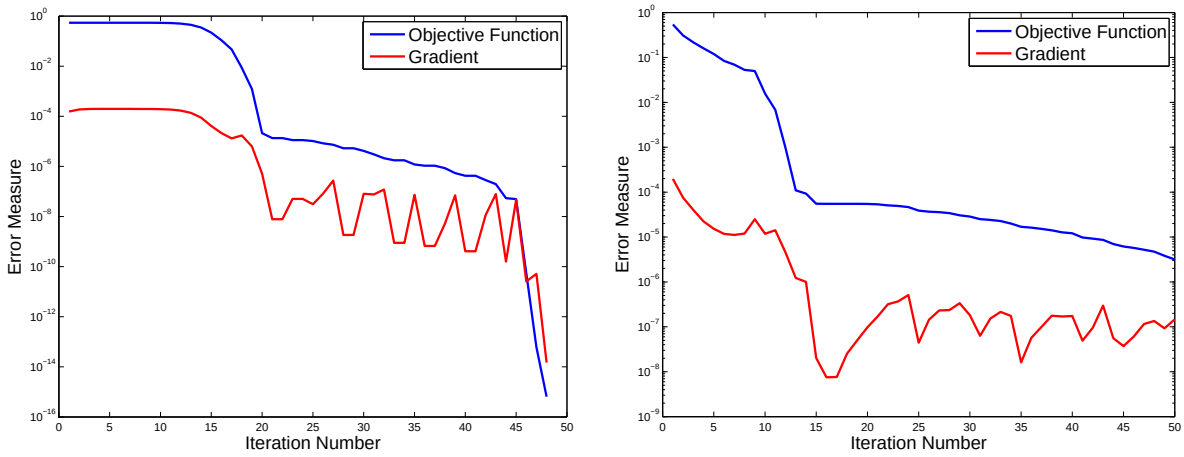

Newton Trust Region BFGS

Figure 3. Convergence history of the material inverse problem on the foam block model.

5 Conclusions

In this report, material inversion algorithms have been presented for viscoelastic materials in the frequency domain. A complete set of first and second order abstract optimization operators for frequency-domain viscoelastic material inversion have been derived from first principles. These operators have been used to compute gradients and Hessians of the Lagrangian which provides a natural interface to an optimization solver. The methods have been implemented in Sierra/SD with an interface to the Rapid Optimization Library (ROL). A foam block model has been used as a demonstration problem for the methods.

References

[1] A. Oberai, N.H. Gokhale, and G.R. Feijoo. Solution of inverse problems in elasticity imaging using the adjoint method. *Inverse Problems*, 19(2):297–313, 2003.

[2] M. Bonnet and A. Constantinescu. Inverse problems in elasticity. *Inverse Problems*, 21(1):R1–R50, 2005.

[3] H.M. Nguyen, O. Allix, and P. Feissel. A robust identification strategy for rate-dependent models in dynamics. *Inverse Problems*, 24(6):1–24, 2008.

[4] J. Janno and L. von Wolfersdorf. An inverse problem for identification of a time and space dependent memory kernel in viscoelasticity. *Inverse Problems*, 17:13–24, 2001.

[5] H. Eskandari, S.E. Salcudean, R. Rohling, and J. Ohayan. Viscoelastic characterization of soft tissue from dynamic finite element models. *Phys. Med. Biol.*, 53:6569–6590, 2008.

[6] H. Yuan and B.B. Guzina. Reconstruction of viscoelastic tissue properties from mr elastography-type measurements. *C. R. Mecanique*, 338:480–488, 2010.

[7] S. Mousavi, D.F. Nicolas, and B. Lundberg. Identification of complex moduli and poisson ratio from measured strains on an impacted bar. *Journal of Sound and Vibration*, 277:971–986, 2004.

[8] W. Rachowicz and A. Zdunek. Application of the fem with adaptivity for electromagnetic inverse medium scattering problems. *Comput. Methods Appl. Mech. Engrg.*, 200:2337–2347, 2011.

[9] M. Bhardwaj, K. Pierson, G. Reese, T. Walsh, D. Day, K. Alvin, J. Peery, C. Farhat, and M. Lesoinne. Salinas: a scalable software for high-performance structural and solid mechanics simulations. In *Supercomputing, ACM/IEEE 2002 Conference*, pages 35–35. IEEE, 2002.

[10] G. Reese, M. Bhardwaj, and T. Walsh. Salinas- theory manual. Technical Report SAND2009-0748, Sandia National Laboratories, 2009.

[11] T. Walsh, W. Aquino, and M. Ross. Source identification in acoustics and structural mechanics using sierra/sd. Technical Report SAND2013-2689, Sandia National Laboratories, 2013.

[12] M. Heroux, R. Bartlett, V. Howle, R. Hoekstra, Hu J., T. Kolda, R. Lehoucq, K. Long, R. Pawlowski, E. Phipps, A. Salinger, H. Thornquist, R. Tuminaro, J. Willenbring, A. Williams, and K. Stanley. An overview of the trilinos project. *ACM Trans. Math. Softw.*, 31(3):397–423, 2005.

[13] T. J. R. Hughes. *The Finite Element Method: Linear Static and Dynamic Finite Element Analysis*. Prentice-Hall, 1987.

[14] L. T. Biegler. *Large-scale PDE-constrained optimization*, volume 30. Springer Verlag, 2003.

[15] J. Nocedal and S. Wright. *Numerical Optimization*. Springer, 2006.

[16] R. D. Cook and M. E. Plesha D. S. Malkaus. *Concepts and Applications of Finite Element Analysis*. John Wiley & Sons, 3rd edition, 1989.

Sandia National Laboratories